

Temperature dependence of d-like surface states on Cu(100) and Cu₃Au(100)-an angle-resolved photoemission study

This article has been downloaded from IOPscience. Please scroll down to see the full text article.

1995 J. Phys.: Condens. Matter 7 2095

(<http://iopscience.iop.org/0953-8984/7/10/016>)

View [the table of contents for this issue](#), or go to the [journal homepage](#) for more

Download details:

IP Address: 171.66.16.179

The article was downloaded on 13/05/2010 at 12:43

Please note that [terms and conditions apply](#).

Temperature dependence of d-like surface states on Cu(100) and Cu₃Au(100)—an angle-resolved photoemission study

R Paniago†, R Matzdorf†, A Goldmann† and R Courths‡

† Fachbereich Physik, Universität GH Kassel, Heinrich-Plett-Straße 40, D-34132 Kassel, Germany

‡ Fachbereich Physik, Universität GH Duisburg, Postfach 10 16 29, D-47048 Duisburg, Germany

Received 20 December 1994

Abstract. We report on the temperature dependence of high-resolution angle-resolved photoemission spectra from d-like (Tamm) surface states on Cu₃Au(100) and Cu(100). The temperature was varied between $T = 39$ and 600 K, the surface states were investigated in the vicinity of the \bar{M} point of the corresponding surface Brillouin zones. On both samples, the temperature influences the Tamm states in a very similar way. We propose that d-like surface states may be used as sensitive probes to monitor the T -dependent potential changes in the outermost layer.

1. Introduction

At the surface of solids, the changed periodicity of the crystal lattice may lead to the development of electronic states not present in the bulk. In the discussion of the surface electronic structure it has become customary to distinguish ‘true’ surface states from surface ‘resonances’ [1–4]. True surface states are located energetically within gaps of the bulk bands projected onto the surface Brillouin zone (SBZ). Resonances are energetically degenerate with bulk bands and therefore it is often not trivial to identify them experimentally. With respect to the angular momentum character, surface states may be classified as ‘Tamm’ (d-like) or ‘Shockley’ (s, p-like) states. The appearance of Tamm states may be visualized as a band-bending effect over the distance of one atomic layer: d-like orbitals, being spatially confined within the outermost lattice plane, can be split off energetically from the bulk states by the action of the surface potential [1, 3, 4]. In contrast, Shockley states arise primarily from the special boundary conditions introduced by the surface. These occur in energy gaps caused by the hybridization of crossed bands in p, s (‘Shockley-inverted’) gaps for which the lower band has odd parity at the zone boundary (p-like), while the upper band is even there (s-like), [1, 2, 4]. Shockley states are damped exponentially into the crystal, but in general extend over a length of several atomic distances. Thus it is evident that Tamm states in particular are very sensitive probes of the electronic charge distribution within the topmost lattice plane. This fact has been realized already [5–9], but only recently experimental work was performed [10–16] to exploit Tamm surface states as sensitive tools to probe the surface potential.

In this paper we present new angle-resolved photoelectron spectra of the well-known [5–12] Tamm state occurring at the \bar{M} point of the SBZ on Cu(100) and of the very similar surface state observed [13–17] on the (100) face of Cu₃Au. In particular we investigate

the dependence of both states on the temperature T of the sample. Our data reveal striking similarities in the T -dependence of both surface states, and we try to give a consistent interpretation with respect to changes of the surface potential.

2. Experimental details

The experiments were performed using a modified ESCA 100 spectrometer from Vacuum Science Workshop Ltd, operated at a base pressure of 4×10^{-11} mbar. It is equipped with a LEED facility, excitation sources for XPS (Mg $K\alpha$, Al $K\alpha$) and UPS (a self-built capillary discharge lamp to excite the Ar I, Ne I, He I and He II emission) and the standard sample preparation techniques. Angular distributions are measured by rotating the crystal through the manipulator axis, thereby keeping the angle between the incident photon beam and the electron take-off direction constant ($\sim 45^\circ$ for UPS results).

The energy resolution of the electron spectrometer could be tuned down to $\Delta E = 20$ meV, as verified by the experimental width of the Fermi edge at $T = 35$ K and by measuring the width of the 3p lines of gaseous argon. The angular resolution $\Delta\theta$ could be modified by an aperture system in front of the electron lens of the analyser. In all cases reported below, the resolution was set to $\Delta\theta = \pm 2^\circ$.

The sample may be heated by a resistance heater up to $T \simeq 700$ K and cooled down by a closed-cycle He refrigerator between room temperature and 35 K. Sample and refrigerator are thermally connected by a flexible copper cable. This connection allows free movement and rotation of the sample manipulator and can be disrupted to achieve temperatures between 300 and 700 K. The temperatures above room temperature could be kept stable to $\Delta T = \pm 10$ K during the time required to take an electron distribution curve.

The samples were cleaned *in situ* by repeated cycles of Ar⁺ sputtering and subsequent annealing up to 640 K (below the order \rightarrow disorder phase transition temperature of Cu₃Au) for several hours. This procedure was done until sharp super-structure LEED spots indicated a well-ordered surface with the sample at room temperature. The intensity of the surface-state emission was also used to monitor the surface quality. The absence of contaminations (typically < 0.01 monolayers) was checked by XPS. The azimuthal orientation was performed using the LEED pattern to an accuracy of $\Delta\varphi < 1^\circ$. The calibration of the polar angle θ was further checked by the observed symmetry around the surface normal ($\theta = 0^\circ$) with $\Delta\theta \leq 1^\circ$.

3. Results and discussion

The connections between 3D real space and 2D reciprocal space dimensions of the (100) surfaces of Cu and Cu₃Au are schematically shown in figure 1. Cu₃Au is composed of alternate layers of pure Cu-like planes, and of planes arranged in a chequerboard pattern with equal numbers of Au and Cu (see the left part of figure 1). Cu(100) is obtained by replacing the Au atoms in Cu₃Au by Cu atoms. Note, however, that the lattice constants are not equal: a (FCC) = 3.61 Å for Cu, while $a = 3.75$ Å for Cu₃Au.

Temperature-dependent photoelectron spectra of the well-known [5–9, 11, 12] Tamm state occurring on Cu(100) about 1.8 eV below E_F at the \bar{M} point of the SBZ are reproduced in figure 2(a). The 3d-like Tamm state is labelled S_1 and its origin is well understood [6]: the \bar{M} point corresponds to the XZW line of the 3D bulk-band structure. Along this line an, absolute energy gap separates the d bands below E_F and the s, p band above E_F by about

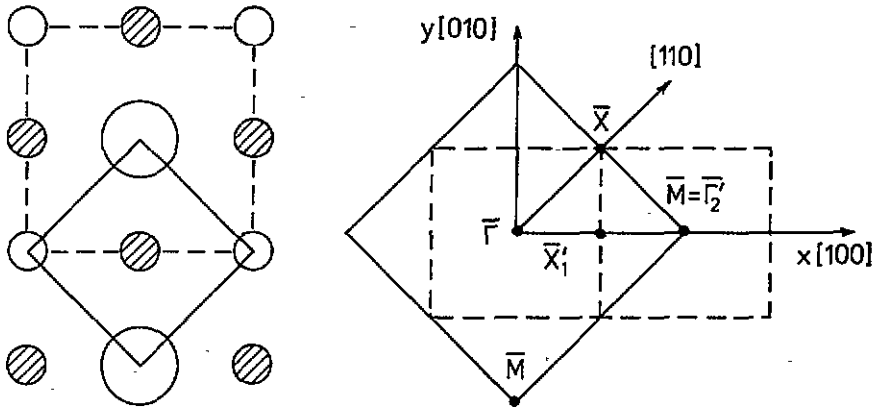


Figure 1. Real-space top view (left) of the Cu₃Au(100) surface: topmost layer with Au and Cu atoms (large and small empty circles) and second layer with only Cu atoms (hatched circles). Cu(100) is obtained after replacement of Au by Cu. The 2D unit cells for Cu(100) and Cu₃Au(100) are indicated by the solid and dashed lines, respectively. Right: corresponding 2D surface Brillouin zones.

4 eV along the entire XZW line. The uppermost *d* band has the orbital symmetry *xy*, if *z* is chosen as the surface normal. This band is almost without dispersion, which indicates that its charge density is localized within the layer, with practically no interaction with the neighbouring layers. A Tamm state on the surface now arises from an excess *s*, *p*-electron density within the outermost plane, splitting a *d*-like surface state off the high density of bulk *d* states along XZW. Inspection of figure 2(a) reveals an interesting dependence on *T*: peak *S*₁ shifts at a rate of $(0.6 \pm 0.1) \times 10^{-4}$ eV K⁻¹, while the bulk state, B (from which *S*₁ is split off), does not move energetically at all. The insensitivity of B to temperature variation results from two compensating effects [19]. When the lattice constant increases due to thermal expansion the initial *d* bands, in general, shift upwards in energy into the direction of *E*_F. Simultaneously, however, the *d*-*d* orbital overlap is reduced and the total *d*-band width decreases. Along XZW, both effects just compensate. In consequence B does not shift despite a thermal lattice expansion, at least in the temperature range of our experiments. We conclude that the energetic shift of *S*₁ with *T* is not due simply to the (trivial) effect of thermal expansion. What we observe is the result of the *T*-dependent variation of the surface potential that splits *S*₁ off the *d* band along the XZW line in 3D *k*-space.

Figure 2(a) shows that the energetic splitting between B and *S*₁ gets smaller at increasing temperature, with a linear dependence on *T*. Simultaneously, the width also increases linearly with *T*. Almost the same decrease of energy distance between B and *S*₁ and the simultaneous increase in linewidth is observed at fixed temperature from samples after gentle argon-ion bombardment and insufficient annealing [21]. This observation strongly suggests that the observed *T*-induced shift might be correlated with the effect of thermal disorder in the surface plane.

In this context it is useful to remember to several earlier studies of the Cu(100)*c*(2 × 2) Au surface [13–16, 22]. After deposition of half a monolayer of gold on the Cu(100) surface at room temperature, Au is incorporated into the outermost layer forming an ordered surface alloy, with a *c*(2 × 2) LEED pattern. This structure of the surface alloy is the same, except for the slightly smaller lattice constant, as that of the first two layers of a (001) surface of

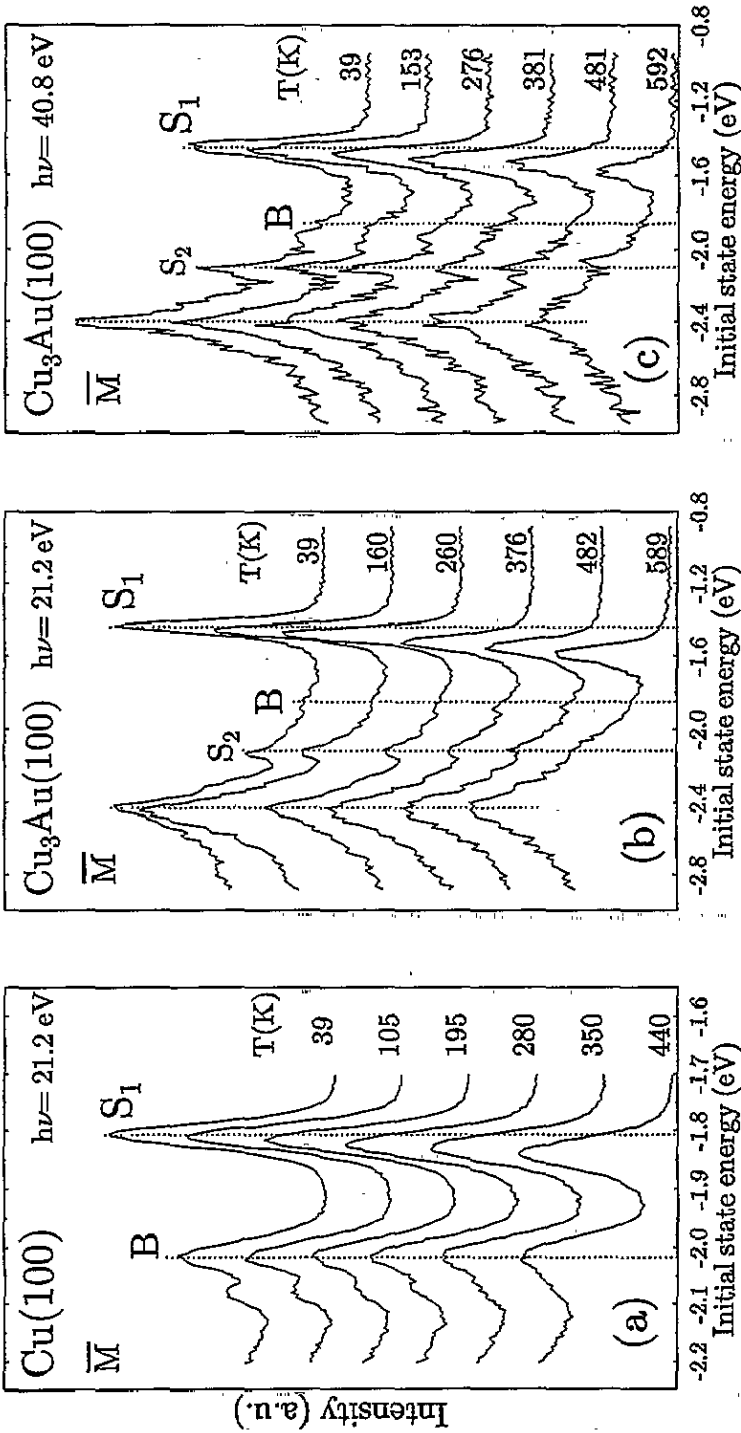


Figure 2. Temperature dependence of photoemission from d-like surface states S_1 around \bar{M} on (a) Cu(100), photon energy $h\omega = 21.2$ eV, (b) $\text{Cu}_3\text{Au}(100)$, $h\omega = 21.2$ eV and (c) $\text{Cu}_3\text{Au}(100)$, $h\omega = 40.8$ eV. The spectra are shifted against each other along the ordinate direction.

Cu_3Au [22]. It is now interesting to monitor the influence of the incorporated Au atoms as a function of Au coverage from zero to 0.5 ML. This has been reported in [15, 16] and some typical results are summarized in figure 3. It shows that the energy position of the Tamm state S_1 at \bar{M} varies linearly with coverage up to the ordered surface alloy. At coverages > 0.5 ML, S_1 shifts back towards the energy position of the clean surface. This is interpreted by a decreasing Au content within the outermost Cu layer, in support of a de-alloying model [15].

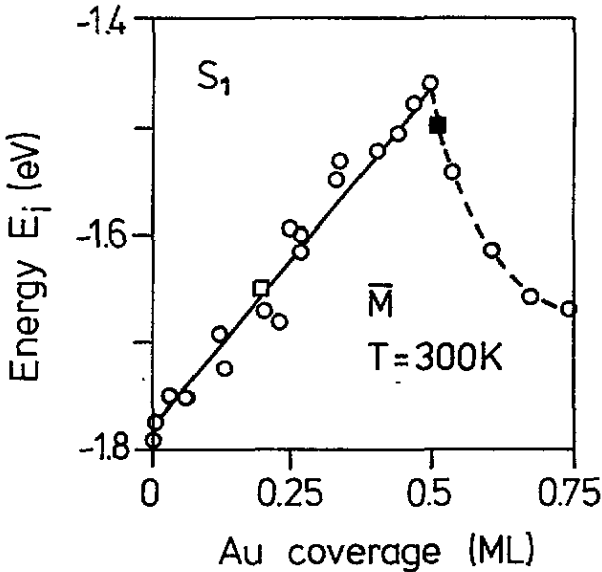


Figure 3. Initial-state energy E_i of the \bar{M} Tamm state S_1 on $\text{Cu}(100)$ versus Au coverage at room temperature, open circles. The filled square shows the corresponding S_1 state on $\text{Cu}_3\text{Au}(100)$.

The shift of S_1 with Au coverage below 0.5 ML can be explained within the framework used for the interpretation of S_1 on $\text{Cu}(001)$: incorporation of Au increases the charge density in the surface plane. Thereby the Coulombic repulsion is enlarged and the $B-S_1$ splitting increases. As reported elsewhere [16] the alloy, i.e. Au in substitutional sites, is already forming below 0.5 ML, even before the $c(2 \times 2)$ LEED pattern is visually observable at about 0.25 ML. The 'hard-sphere' diameters of Au (lattice constant $a = 4.09 \text{ \AA}$) and Cu ($a = 3.61 \text{ \AA}$) differ considerably. Therefore, aside from the experimentally observed [22] buckling (with the Au atoms located 0.1 \AA outwards from the Cu atoms and the distance between the mixed top layer and the second all Cu layer expanded by 4.2% with respect to the bulk) we must in particular expect a considerable lateral distortion of the C_{4v} surface point group symmetry. Thus we believe that the linear dependence observed in figure 3 is due to the combined effect of adding charge density and inducing structural disorder. This idea is also compatible with experiments reported for a $\text{Cu}_{90}\text{Au}_{10}(100)$ random alloy. It exhibits about 20% Au surface concentration and shows a shift of S_1 to $E_i = -1.65 \text{ eV}$ [23]. This data point is included as an open square in figure 3 and fits perfectly into the linear dependence [16, 23]. If our interpretation is correct, and not only the different chemical environment but also the considerable geometrical disorder contribute to the shift observed in figure 3, we end up with the conclusion that disorder tends to weaken the effect

of the surface potential, thereby reducing the energetic distance of S_1 from the bulk states it originates from.

As already mentioned, the Cu(100)c(2 × 2) Au surface alloy is geometrical almost identical to the outermost two layers of Cu₃Au(100), if this bulk alloy is terminated with the Cu₅₀Au₅₀ layer, compare figure 1. Returning our attention to figure 2(b), which shows the angle-resolved photoemission at $\vec{M} = \vec{\Gamma}'_2$ from Cu₃Au(100) at a photon energy $\hbar\omega = 21.2$ eV, we detect the Tamm state S_1 around $E_i = -1.50$ eV. Its initial-state energy observed at room temperature is included in figure 3 as a filled square, and it fits perfectly the data related to Cu(100)c(2 × 2) Au. This result was to be expected from considerations outlined above, and had been observed already [14–17]. Note in passing that this excellent agreement gives conclusive evidence that the Cu₃Au(100) surface as prepared in our experiments shows indeed a Cu(100)c(2 × 2) Au-like termination. This geometry seems to be favoured thermodynamically as compared with a termination by a pure copper layer: the identical conclusion was arrived at also by ion-scattering experiments [24] and the analysis of angle-dependent core-level photoemission intensities [25].

Next, we concentrate on the temperature dependence of S_1 in figure 2(b). We clearly observe three effects. First, increasing T reduces the energy splitting between S_1 and the corresponding bulk-band edge. The latter has been identified in bulk-band-mapping experiments [20] to be located at $E_i = -1.80$ eV and is labelled B in figure 2(b). The position of S_1 in its dependence on T is more clearly seen in the upper panel of figure 4. In contrast to S_1 on Cu(100), where a linear shift of E_i with T was found up to $T = 600$ K [8, 21], we observe an increasing negative slope already between 400 and 500 K. We interpret this fact via an increase of (geometrical) lattice disorder when T approaches the (chemical) order → disorder phase transition at 663 K. As is also clearly evident from figure 2(b), we observe a loss in amplitude with rising T . The detailed analysis shows that it is linear within statistical scatter of the data and may well be described by $A(T) = A(0)(1 - bT)$, with $b = (9.2 \pm 0.4) \times 10^{-4} \text{ K}^{-1}$. This means an amplitude decrease by about a factor of two within 600 K and is comparable in magnitude to the behaviour of S_1 on Cu(100) [8, 21]. It may be interpreted by electrons scattered out of the detector solid angle by coupling to acoustical phonons. This mechanism has been demonstrated to explain the temperature-dependent intensities of bulk-band photoemission quite well [26] and it should be operative in surface-state emission as well. Finally we observe that the experimental total width Γ_{exp} of S_1 on Cu₃Au(100) is almost independent of T (see the lower panel of figure 4), Γ_{exp} changes from (93 ± 5) meV at 40 K to only (100 ± 5) meV at 600 K. This behaviour is in contrast to that of S_1 on Cu(100), which shows $\Gamma_{\text{exp}} = (47 \pm 5)$ meV at 40 K and (68 ± 5) meV at 500 K, i.e. an increase by nearly 50%. We must conclude that Γ_{exp} on Cu₃Au(100) is not dominated by temperature effects. At present we are not able to offer a unique interpretation for that. One plausible argument may be that the presence of the Au atoms increases the density of s, p-like electrons in the vicinity of the electron hole left by photoemission from S_1 . Consequently, the shortened hole lifetime gives a larger contribution to Γ_{exp} as compared with that for clean Cu(100). However, broadening may also be caused by changes of the ‘perfect’ stoichiometry within the outermost plane of Cu₃Au. Figure 3 indicates both some excess Au atoms (remaining after the sputter-annealing process) or some missing Au atoms can also induce significant contributions to the experimentally observed width Γ_{exp} .

Besides S_1 , a second weaker peak, S_2 (labelled S_3 in [20]), is observed at $E_i \simeq -2.1$ eV. Calculations indicate that it is due to a surface resonance [20]. The distance between S_1 and S_2 is predicted [20] to be 0.54 eV, in good agreement with 0.65 eV observed in our work at 39 K. To check for its surface character we have studied S_2 (and also S_1 , of course)

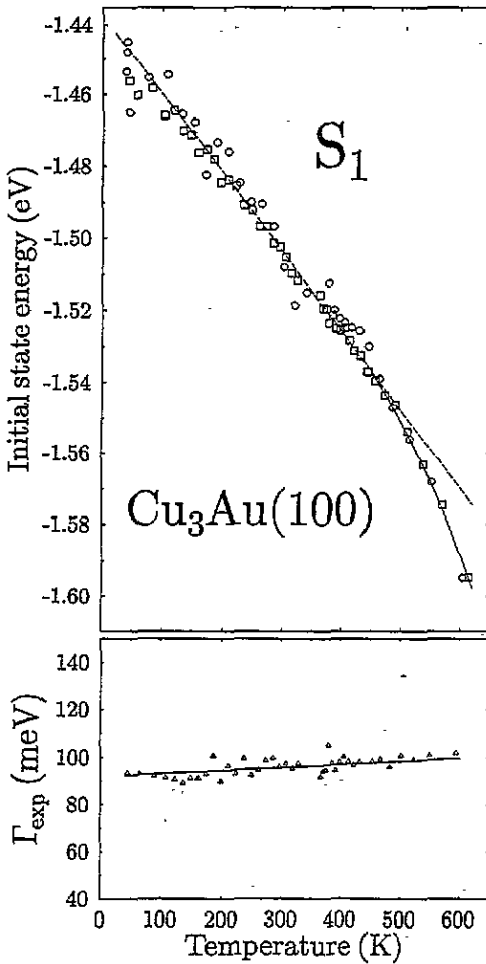


Figure 4. Top panel: initial-state energy E_i of the Tamm state S_1 observed on $\text{Cu}_3\text{Au}(100)$ versus sample temperature. Bottom panel: experimental full width at half maximum Γ_{exp} of the same state versus temperature.

at different photon energies: $\hbar\omega = 21.2$ eV (He I), 16.8 eV (Ne I) and 40.8 eV (He II). Sample spectra taken with HeII radiation are reproduced in figure 2(c). No energy dispersion with $\hbar\omega$ is observed, a necessary condition for surface states and surface resonances. As figures 2(b) and 2(c) also clearly show, the position of S_2 does not shift as strongly with T as S_1 does. This seems reasonable: being a surface resonance, S_2 probably extends several layers deep into the crystal. Therefore its sensitivity to T -dependent potential changes within the outermost layer is much smaller than for S_1 . From angle-dependent spectra we have also determined the energy dispersion $E_i(k_{\parallel})$ along $\bar{\Gamma}\bar{M}$ of both S_1 and S_2 . The results are summarized in figure 5. We hope that these data may stimulate more detailed theoretical investigations.

Although $\text{Cu}(100)$ and $\text{Cu}_3\text{Au}(100)$ differ considerably in their surface geometry, the corresponding surface states labelled S_1 in figure 2 show very similar behaviour with sample temperature. Several arguments have been given above that the reduced shift S_1 off the parent bulk bands with increasing temperature might be due to lateral (thermal) disorder.

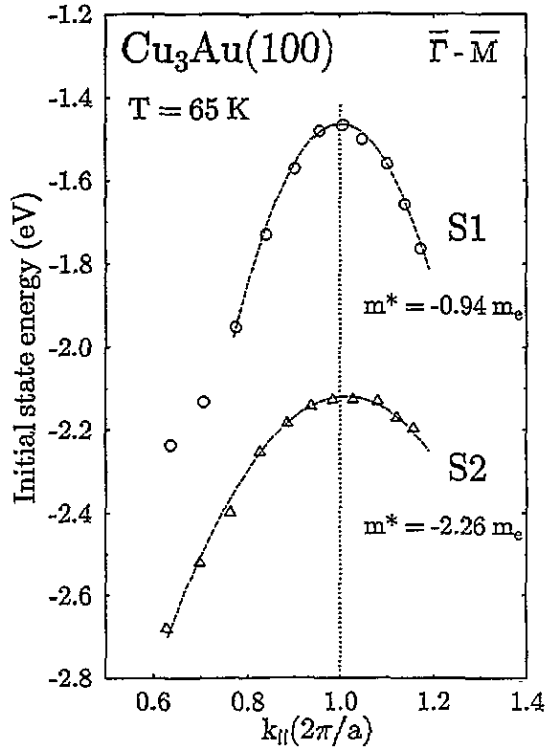


Figure 5. Dispersion $E_1(k_{||})$ of the surface bands S1 and S2 observed on $\text{Cu}_3\text{Au}(100)$ along the $[100]$ direction of the surface Brillouin zone. Sample temperature $T = 65$ K.

No detailed theory is available yet. To mimic thermal disorder, we have investigated a linear chain model. By numerical integration of the Schrödinger equation we were able to identify a 1D 'surface' state. Introduction of static geometrical disorder (statistically arranged variations of the 1D lattice constant) in fact shifts the surface state in energy, without inducing energetic broadening. These simple model calculations thus seem to support the idea that thermal disorder in the surface plane of $\text{Cu}(100)$ and $\text{Cu}_3\text{Au}(100)$ may weaken the splitting of S_1 off the bulk states. Of course, realistic calculations are required to understand what really happens. Nevertheless we communicate our data since they clearly demonstrate the use of surface-localized Tamm states as very specific and very sensitive probes of the influence of temperature on the potential in the surface.

Acknowledgment

Our work is continuously supported by the Deutsche Forschungsgemeinschaft (DFG).

References

- [1] Kevan S D (ed) 1992 *Angle-Resolved Photoemission: Studies in Surface Science and Catalysis* vol 74 (Amsterdam: Elsevier) and references therein
- [2] Smith N V 1985 *Phys. Rev. B* **32** 3549

- [3] Davison S G and Steslicka M 1992 *Basic Theory of Surface States* (Oxford: Clarendon)
- [4] Forstmann F 1993 *Prog. Surf. Sci.* **42** 21
- [5] Gay J G, Smith J R and Arlinghaus F J 1979 *Phys. Rev. Lett.* **42** 332
- [6] Heimann P, Hermanson J, Miosga H and Neddermeyer H 1979 *Phys. Rev. Lett.* **42** 1782; 1979 *Phys. Rev. B* **20** 3059
- [7] Heimann P, Hermanson J, Miosga H and Neddermeyer H 1979 *Phys. Rev. Lett.* **43** 1757
- [8] Kevan S D and Shirley D A 1980 *Phys. Rev. B* **22** 542
- [9] Westphal D and Goldmann A 1980 *Surf. Sci.* **95** L249
- [10] Pessa M, Asonen H, Rao R S, Prasad R and Bansil A 1981 *Phys. Rev. Lett.* **47** 1223
- [11] Wincott P L, Brookes N B, Law D S-L and Thornton G 1986 *Phys. Rev. B* **33** 4373
- [12] Wincott P L, Law D S-L, Brookes N B, Pearce B and Thornton G 1986 *Surf. Sci.* **178** 300
- [13] Hansen J C, Benson J A, Clendening W D, McEllistrem M T and Tobin J G 1987 *Phys. Rev. B* **36** 6186
- [14] Graham G W 1987 *Surf. Sci.* **184** 137
- [15] Hansen J C and Tobin J G 1989 *J. Vac. Sci. Technol. A* **7** 2475
- [16] Hansen J C, Wagner M K and Tobin J G 1989 *Solid State Commun.* **72** 319
- [17] Löbus S, Lau M, Courths R and Halilov S 1995 *Surf. Sci.* at press
- [18] Eckardt H, Fritsche L and Noffke J 1984 *J. Phys. F: Met. Phys.* **14** 97
- [19] Knapp J A, Himpfel F J, Williams A R and Eastman D E 1979 *Phys. Rev. B* **19** 2844
- [20] Löbus S, Courths R, Halilov S, Gollisch H and Feder R 1995 *Surf. Rev. Lett.* at press
- [21] Matzdorf R, Meister G and Goldmann A 1993 *Surf. Sci.* **286** 56
- [22] Wang Z Q, Li Y S, Lok C K C, Quinn J and Jona F 1987 *Solid State Commun.* **62** 181
- [23] Asonen H, Barnes C J, Pessa M, Rao R S and Bansil A 1985 *Phys. Rev. B* **31** 3245
- [24] Niehus H and Achete C 1993 *Surf. Sci.* **289** 19
- [25] Stuck A, Osterwalder J, Schlapbach L and Poon H C 1991 *Surf. Sci.* **251/252** 670
- [26] Matzdorf R, Meister G and Goldmann A 1993 *Surf. Sci.* **296** 241